ORIGINAL ARTICLE

Finite element modeling of maximum stress in pelvic floor structures during the head expulsion (FINESSE) study

Hana Cechova[1] · Vladimir Kalis[2,3,4] · Linda Havelkova[1] · Zdenek Rusavy[2,3,4] · Pavel Fiala[5] · Martina Rybarova[5] · Ludek Hyncik[1] · Ladislav Krofta[6] · Khaled M. Ismail[3,4] (ORCID)

Abstract

Introduction and hypothesis Several studies have assessed birth-related deformations of the levator ani muscle (LAM) and perineum on models that depicted these elements in isolation. The main aim of this study was to develop a complex female pelvic floor computational model using the finite element method to evaluate points and timing of maximum stress at the LAM and perineum in relation to the birth process.

Methods A three-dimensional computational model of the female pelvic floor was created and used to simulate vaginal birth based on data from previously described real-life MRI scans. We developed three models: model A (LAM without perineum); model B (perineum without LAM); model C (a combined model with both structures).

Results The maximum stress in the LAM was achieved when the vertex was 9 cm below the ischial spines and measured 37.3 MPa in model A and 88.7 MPa in model C. The maximum stress in the perineum occurred at the time of distension by the suboocipito-frontal diameter and reached 86.7 MPa and 119.6 MPa in models B and C, respectively, while the stress in the posterior fourchette caused by the suboccipito-bregmatic diameter measured 36.9 MPa for model B and 39.8 MPa for model C.

Conclusions Including perineal structures in a computational birth model simulation affects the level of stress at the LAM. The maximum stress at the LAM and perineum seems to occur when the head is lower than previously anticipated.

Keywords Birth · Delivery · Levator · Modeling · Muscle · Partum · Perineal · Stress · Tension

Hana Cechova, Vladimir Kalis and Linda Havelkova are joint first authors.

✉ Khaled M. Ismail
khaled.ismail@lfp.cuni.cz

[1] New Technologies - Research Centre, University of West Bohemia, Pilsen, Czech Republic

[2] Department of Obstetrics and Gynecology, University Hospital, Pilsen, Czech Republic

[3] Department of Obstetrics and Gynecology, Faculty of Medicine, Charles University, alej Svobody 76, 304 60 Pilsen, Czech Republic

[4] Biomedical Center, Faculty of Medicine in Pilsen, Charles University, Pilsen, Czech Republic

[5] Department of Anatomy, Faculty of Medicine in Pilsen, Charles University, Pilsen, Czech Republic

[6] Institute for the Care of Mother and Child, Podolské nábřeží 157, 147 00 Prague, Czech Republic

Introduction

Vaginal birth causes a significant degree of deformation to the levator ani muscle (LAM) and perineum including the anal sphincter complex. Trauma to the pelvic floor can have a short- and long-term negative impact on a woman's quality of life including increasing her risk for urinary or anal incontinence, perineal pain, dyspareunia and symptoms of pelvic organ prolapse [1–4]. Therefore, the thorough analysis of the actual components of birth and the evaluation and quantification of their impact on the pelvic floor are of paramount importance to understand the underlying mechanism of such deformation. Furthermore, a focus on understanding the timing(s) and site(s) of maximal deformation and displacement is an essential prerequisite to find solutions to mitigate the risk of adverse outcomes.

In the clinical setting, quantification of the deformation of the external visible structures is achieved by means of manual, stereo-video or photo documentation assessments [5–7]. However, the precise direct measurement of deeper layers is

a serious limitation of real-life measurements. Therefore, recently several research groups have focused on using finite element models based on available anatomical and biomechanical data [8–16]. This technology has been used to assess the impact of certain obstetric maneuvers and interventions on the level of strain of pelvic floor structures. However, more recent advancements in computational science and biomechanical material simulation have facilitated the refinement of such models, making them more realistic and ready for testing.

The majority of studies have assessed LAM and perineal muscle deformations on models that depicted these elements in isolation [8–14, 16, 17]. These studies reported an LAM stretch ratio ranging between 1.63 and 3.5:1 [8, 9]. The maximum LAM stretch was reported to occur when the leading margin of the fetal head was between 5 and 11 cm below the level of the ischial spines [9, 15, 17, 18]. Jing et al. developed a model incorporating the LAM and perineum. However, the perineum was modeled as a simplified structure integrated within that of the LAM. In their study, the maximum stretch ratios for the LAM and perineum were 4.64 and 4.15:1, respectively. These values varied with the alteration in the stiffness of the modeled perineum. Moreover, their reported maximum LAM stretch was achieved when the tip of the head reached 12.2 cm along the curve of Carus [10].

Hence, the main aim of this study was to develop a complex female pelvic floor computational model using the finite element method and use it to simulate vaginal birth evaluating the points of maximum stress at the LAM and perineum (i.e., perineal muscles, perineal membrane and overlying skin) and the timing of their occurrence in relation to the process of birth. As a secondary aim, we wanted to assess the impact of the presence of perineal structures and the anococcygeal ligament on LAM stress and vice versa by assessing the same parameters on more simplified models of the perineum or LAM only.

Methods

A three-dimensional computational model of the female pelvic floor was created and used to simulate vaginal birth. The model was based on live-subject MRI data (a 25-year-old nulliparous woman with a BMI of 21.9 kg/m^2 and no pelvic floor dysfunction symptoms or displacement) using 130 previously described axial 3-T MR images [15, 18]. The initial geometry was reconstructed using free semiautomatic 3D-Slicer software (3.0, BWH, Boston, MA, USA). The resulting geometry and mesh were created in HyperMesh commercial software (11.0, Altair, MI, USA). The final simulation was performed using Virtual Performance Solution commercial software (15.0; ESI Group, Paris, France).

Developing the biomechanical model of the fetal head

The fetal head and its trajectory through the pelvic floor structures followed those described by dynamic magnetic resonance of a vaginal delivery [19]. However, the fetal head was scaled up to ensure that its main dimensions corresponded to those of an average-size term fetus.

Developing the biomechanical model of bony pelvis and levator ani muscles

The bony pelvis and the three components of the LAM (pubovisceral muscle, PVM; puborectal muscle, PRM; iliococcygeus muscle, ICM) were adapted from our previous modeling study using MRI data as well [15, 18]. The pelvis was constructed with 2D triangular mesh as a rigid non-deformable body, while the deformable muscle was modeled by 3D tetrahedral mesh.

During vaginal birth, the LAM undergoes extremely large deformation [8, 10, 15, 17, 18]. Therefore, similar to our previous studies and using the same parameters, the hyperelastic nonlinear Ogden material model was used [18, 20]. The material parameters were based on experimental measurements of porcine muscle samples. Twenty LAM samples from ten female pigs were measured (age: 12–14 weeks, weight: 33–45 kg, nulliparous). The muscles were cleared of fascia and cut into cuboid-shaped samples suitable for the measurement. Each sample underwent preconditioning consisting of 20 cycles up to 15% of the sample relaxed length after excision, freezing, thawing and clamping in the measurement device as previously described [18, 21]. The uniaxial mechanical test was performed using the Zwick/Roell Z050 traction machine (Zwick/Roell, Ulm, Germany). The extension continued until the muscle ruptured. The tensile forces and sample elongation were recorded. To identify the unknown parameters of the Ogden model, we estimated the stress-strain characteristics using these recordings by fitting two pairs of material constants μ and α. The following values of the Ogden parameters were used: $\mu1 = 8.9$ GPa; $\mu2 = 21.6$ GPa; $\alpha1 = 0.1803$; $\alpha2 = 15.112$. The detailed process of material parameter identification was described in a previous publication [18]. The muscle tissue density and Poisson's ratio used were $\rho = 1.06$ kg/l and $\nu = 0.499$, respectively [22, 23].

Developing the biomechanical model for perineal structures

The main perineal structures, such as the transverse perineal muscle, bulbospongious muscle, ischiocavernous muscle, anoccocygeal ligament, perineal membrane, anal sphincter complex and perineal skin, were newly developed for this study. To design these components, the geometry as well as

material parameters were based on available data from previous experimental, clinical and biomechanical studies [6, 7, 24–27] as well as cadaveric measurements. For this study, six embalmed cadaver pelvises were used with a mean age of 69.2, SD = 5.6. The preparations were obtained from the Department of Anatomy at the Faculty of Medicine in Pilsen, Charles University. Each of the donors had signed informed consent forms for the donation of their body tissues to the Faculty of Medicine in Pilsen for research and educational purposes. Cadavers were treated according to local standard fixation methods. After placement in embalming fluid (10% formalin, 70% ethanol and 20% glycerine), the preparations were switched to 70% ethanol. Once differentiated and photographed, the prepared muscles were measured in situ using calipers. Measured values included total muscle length, muscle belly width and dimensions of muscular attachment. Significant outliers of shape of muscle bellies were eliminated from the study. This methodology was chosen because of the lack of reliable and comprehensive data from imaging studies about these structures as highlighted by several authors [9, 10, 16].

All perineal muscles, as well the anococcygeal ligament, were modeled by the Ogden material model to ensure they could cope with the large deformations occurring during vaginal delivery. For the perineal muscles, we used the same material constants as for LAM modeling. However, for the anococcygeal ligament, the material parameters were based on data available in the literature [24]. The perineal membrane was modeled as a layered membrane, and the material parameters were adapted from previously published information [25]. The layered membrane was composed of the matrix and two layers of fibers in perpendicular directions. The perineal skin model was based on an elastic shell; the material parameters were in line with those published by Long et al. [26]. The dimensions and positioning of most of perineal structures were based on cadaveric measurements. Those of the anal sphincter were determined from a 3D ultrasound scan volume of a primiparous woman participating in another clinical study. This was deemed suitable as measurements do not seem to be affected by birth [27]. Anal sphincter volume was acquired transperineally in the supine position using a GE Voluson E8 (GE Kretz Medizintechnik, Zipf, Austria) with an 8–4-MHz curved array volume transducer (acquisition angle 85°). Volume acquisition was performed at rest and maximal squeeze.

Boundary conditions

Some surrounding tissues were not represented and replaced by boundary conditions to ensure the realistic behavior of represented parts. The pelvis was fixed for all degrees of freedom to fit the whole model in space. In our model, the ICM attachment to the arcus tendineus fasciae pelvis was replaced by fixation of this area in the superior-inferior direction. The PVM attachment was replaced by full fixation of this muscle part and its connection to the ICM was not implemented. The PRM normally originates from the inferior part of the pubic symphysis and forms a sling around the rectum. This connection was modeled by two boundary conditions where the origin was fixed for all degrees of freedom, and the lower arch of muscle was firmly connected to the external anal sphincter.

The areas of perineal muscle attachments were fixed respecting the real anatomy [3, 8].

Anatomically, the superficial transverse perineal muscles originate from the ischial rami and are inserted into the perineal body. In this model, the attachment to the pelvis was modeled by full fixation of this part in space. The connection to the perineal body was replaced by the interference fit to this tissue. The bulbospongious muscle origins are in the perineal body and are inserted into the pubic arch, fascia of corpora cavernosa and clitoris. Their close connection with the perineal body was also replaced by interference fit and the insertion was modeled by fixation to the pubic arch. The same principle of fixation was used for the ischiocavernous muscles, which originate from the ischial tuberosities and rami on either side and are inserted into clitoris. With respect to anatomy, the anococcygeal ligament was fixed in all degrees of freedom in its attachment to the coccyx and connected to the external anal sphincter. The interference fit was also modeled between the external and internal anal sphincters and for the other connections such as the perineal membrane and perineal muscles. In addition, the perineal membrane was also fully fixed along the sides to simulate the connection to the inferior pubic ramus. The perineal skin was connected to the perineal muscles by linked elements to substitute connective tissues.

Simulations

The vaginal delivery of the fetal head was simulated using the developed finite element model and the Virtual Performance Solution commercial software (15.0; ESI Group, Paris, France). The same fetal head and birth trajectory were used for all three models to facilitate comparison. No obstetric interventions or maneuvers were simulated, i.e., all simulations were "hands off" (Video). We measured the site, absolute values and timing of points of maximum stress in the LAM and perineum in relation to the course of vaginal birth. The timing of the maximum LAM values was defined by stations, i.e., the head descent measured between the most distal point of the fetal head and the level of the ischial spines as previously described by Krofta et al. [15]. The timing of the maximum perineal stress values was defined by the fetal head diameter passing the plane between the lower margin of the pubic bone and posterior fourchette [12, 13]. Finally, the downward displacement of the LAM and perineal structures were compared to their pre-delivery position [15, 18].

For the purpose of this study we developed three models: model A (LAM without perineum); model B (perineum without LAM); model C (a combined model with both structures) (Fig. 1a–d). Due to the nature of this computational study, a sample size calculation and advanced statistics were not applicable.

Results

This study revealed that the maximum stress in the LAM was in the anterior portion of the PVM. It measured 37.3 MPa in model A and 88.7 MPa in model C. This stress was achieved when the vertex was 9 cm below the ischial spines (Fig. 2a–c). The maximum downward displacement of the PVM at the level of the vagina was 0.2 cm and 2.4 cm in models A and C, respectively, while the maximum downward displacement of the PVM at the level of the rectum was 0.6 cm in model A and 1.3 cm in model C (Table 1).
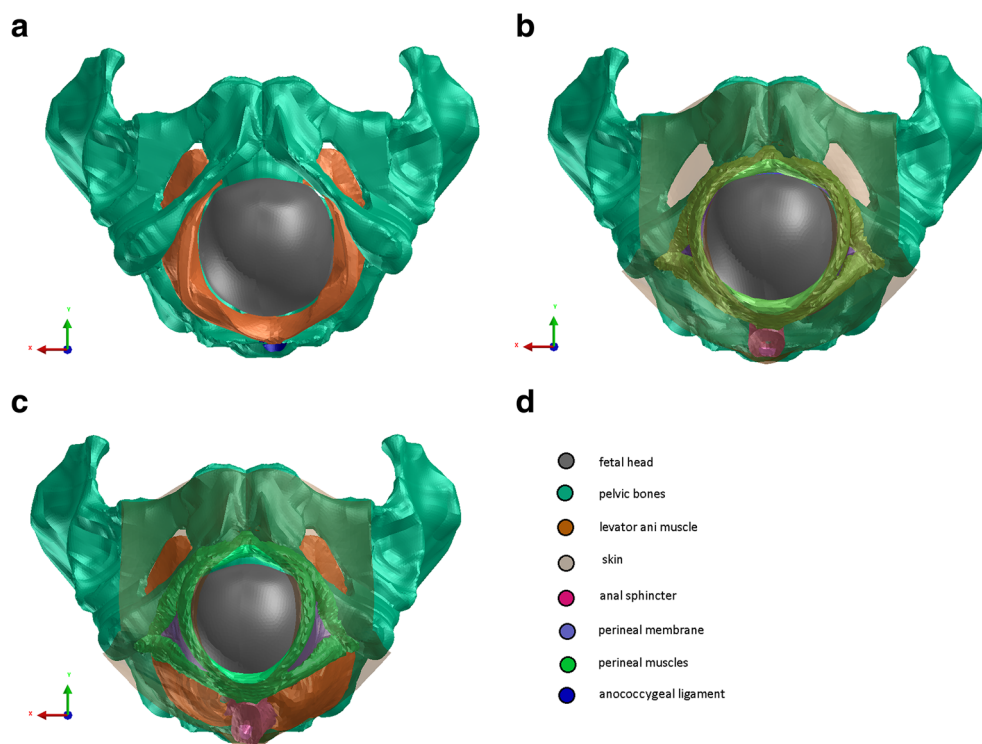
The maximum stress at the perineal body was found in the area of the posterior fourchette and was caused by the suboccipito-frontal diameter. The maximum measurements were 86.7 MPa and 119.6 MPa in models B and C, respectively. The distal displacement was 4.9 cm in both models (Table 2). The stress level in the posterior fourchette when the suboccipito-bregmatic diameter was distending the perineum was 36.9 MPa for model B and 39.8 MPa for model C.

Discussion

Summary of findings

The aim of this study was to develop a complex pelvic floor finite element model to assess the impact of head expulsion on the LAM and perineum in isolation with all structures represented. Hence, we were able to analyze the behavior of both structures separately and compare these data with those obtained from the complex model. We found that the LAM maximum stress markedly differed between the model with LAM only (model A) and the complex model (model C). However, the difference was not as marked when comparing stress at the perineum between models B and C. Therefore, it is imperative that any future computational modeling to assess the impact of childbirth on LAM must be done on a model equipped with both LAM and perineal elements. Our study was designed to explore whether there were differences in LAM stress in the LAM-only compared to a more realistic computational model and not to assess the reasons for any identified differences. Nevertheless, we believe that the observed difference in the measured LAM stress between models A and C is interesting. Although only speculative, it is possible that some of the tension that occurs at the LAM during birth is secondary to the traction force from the displacement of superficial layers, which is transmitted to the LAM through its ligamentary attachments.

Fig. 1 Variants of the model. **a** Model A: LAM without perineum. **b** Model B: Perineum without LAM. **c** Model C: Combined model containing both LAM and perineum. **d** Color legend

fetal head
pelvic bones
levator ani muscle
skin
anal sphincter
perineal membrane
perineal muscles
anococcygeal ligament

Table 1 Measured values at the time of maximum stress in the LAM in models A and C

	Model A (LAM)	Model C (LAM)	Difference model C/A
Location (anatomical description or some coordinates)	Antero-inferior margin	Antero-inferior margin	None
Maximum stress (MPa)	37.3	88.7	2.4-fold
Timing: head descent/station (cm)	+9.1	+8.9	0.98-fold
Downward displacement of PVM at level of vagina (cm against resting position)	0.2	2.4	12-fold
Downward displacement of PVM at level of rectum (cm against resting position)	0.6	1.3	2.1-fold

We were able to assess the station of the fetal head associated with the maximal LAM stress. Interestingly, this seemed to happen when the baby's zygomatic processes of the temporal bones were at the level of the maternal ischial spines (Fig. 2a) and hence much lower than we previously expected. This implies that attempts to reduce pressure on pelvic floor structures before crowning of the perineum are probably of limited protective value and strengthens the view that interventions to reduce such pressure at the time of head crowning might be useful, not only for the perineum but also for the LAM. Furthermore, based on the previously described real-life fetal head trajectory [19], we identified that the maximum stress at the perineum is caused by the suboccipito-frontal rather than the suboccipito-bragmatic diameter secondary to the natural head extension as the subocciput pivots against the maternal symphysis pubis. This suggests that, in the clinical setting, manual perineal support at the time of head expulsion should be maintained at least till the supraorbital margin of the frontal bone passes the posterior fourchette.

Comparison of findings to other studies

Several of the computational models used to describe deformations of the LAM during vaginal birth were not equipped with a perineum [8, 9, 14, 16]. Although Jing et al. developed a model incorporating an LAM and perineum, the latter was developed as a simplified structure within the levator [10]. Furthermore, our previous computational modeling studies involved only modeling of the perineal structures without the LAM [11–13]. Based on the differences we identified in the maximum stress between models A and B compared to C, the reported previous measurements might not have been

Fig. 2 Fetal head position at the time of maximum stress in the LAM in model C. **a** Relationship between the fetal head and level of ischial spines. **b** Obstetrician's view at the time of maximum stress in the LAM. **c** Obstetrician's view at the time of maximum stress in the LAM with all structures superficial to the LAM not demonstrated to facilitate its visualization
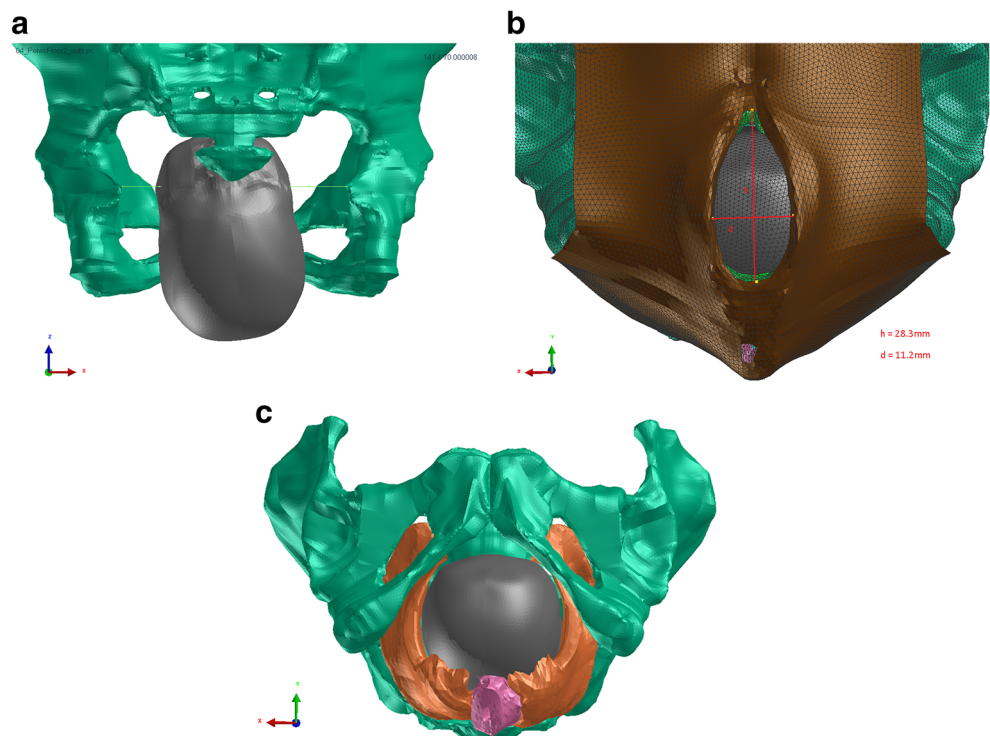
Table 2 Measured values at the time of maximum stress in perineal structures in models B and C

	Model B	Model C	Difference model C/B
Location in the perineal body (Anatomical description)	Posterior fourchette	Posterior fourchette	None
Maximum stress (MPa)	86.7	119.6	1.4-fold
Timing: passing fetal head circumference [anatomical description]	Suboccipito-frontal	Suboccipito-frontal	None
Caudal displacement (cm against resting position)	4.9	4.9	None

precise particularly for the maximum LAM stress. Nevertheless, our findings concur with the results of these studies in that the point of maximum LAM stress seems to occur in the anterior portion of the PVM [8–10, 15, 17, 18]. We identified that the LAM maximum stress was achieved when the leading edge of the head was at 9 cm below the level of the ischial spines. Interestingly, Jing et al. reported the maximum stretch when the tip of the head was 12.2 cm along the curve of Carus [10]. It is important to emphasize that our measurement was based on the vertical distance from the ischial spines rather than the distance along the birth trajectory.

Strengths and limitations

We appreciate that there are some limitations to our study. First, the muscles material properties were based on uniaxial testing of porcine LAM after preconditioning. Furthermore, our cadaveric measurements were taken from an older cohort of women. These properties and measurements may differ from those of a younger pregnant woman particularly as they only represent the muscle rather than the pelvic diaphragm (LAM together with its superior and inferior fascia) and do not consider the impact of pregnancy hormones on muscles and connective tissue. It is possible that these issues could have affected the accuracy and realism of our model. However, for ethical reasons, obtaining such parameters from women in the childbearing age was not feasible. Second, in the dynamic MRI real-time fetal head trajectory we used [19], there was a degree of left asynclitism (Fig. 2a) that seemed to persist throughout this delivery. This is probably the reason why measured stresses on the left and right side of the LAM and perineum were not symmetrical. Due to this left asynclitism, the highest LAM stress was measured on the left side. It is possible that if the fetal head passed the pelvic floor synclitically, the maximum stress might have been lower. Finally, we did not assess the realism of the model by comparing the calculated levels of strain with actual anatomical displacement data obtained from real-time imaging of the birth process. However, to our knowledge such data are not readily available yet. It would be prudent to explore the feasibility of such comparisons in future validation studies of our model. Nevertheless, our ability to develop a finite element model that depicts both the LAM and perineal components with realistic material properties and utilizing dimensions and trajectories based on real-life MRI images are major strengths to our work.

Conclusion

Including the perineal structures in a computational model seems to affect the maximum LAM stress. Moreover, the maximum stress at the LAM and perineum seems to occur when the fetal head is lower than anticipated. Due to the novelty of our results, it is important for these findings to be assessed in future independent studies using different birth trajectories, fetal head dimensions and positions.

Declarations

Ethical approval Ethical approval was not required for this computational modeling study. Consent related the use of cadavers was described in the methods section.

References

1. Blomquist JL, Muñoz A, Carroll M, Handa VL. Association of delivery mode with pelvic floor disorders after childbirth. JAMA-J Am Med Assoc. 2018;320:2438–47. https://doi.org/10.1001/jama.2018.18315.

2. Necesalova P, Karbanova J, Rusavy Z, et al. Mediolateral versus lateral episiotomy and their effect on postpartum coital activity and dyspareunia rate 3 and 6 months postpartum. Sex Reprod Healthc. 2016;8:25–30. https://doi.org/10.1016/j.srhc.2016.01.004.

3. Larson KA, Yousuf A, Lewicky-Gaupp C, et al. Perineal body anatomy in living women: 3-dimensional analysis using thin-slice magnetic resonance imaging. Am J Obstet Gynecol. 2010;203:494.e15–21. https://doi.org/10.1016/j.ajog.2010.06.008.

4. Handa VL, Roem J, Blomquist JL, et al. Pelvic organ prolapse as a function of levator ani avulsion, hiatus size, and strength. Am J Obstet Gynecol. 2019;221:41.e1–7. https://doi.org/10.1016/j.ajog.2019.03.004.

5. Rizk DEE, Thomas L. Relationship between the length of the perineum and position of the anus and vaginal delivery in Primigravidae. Int Urogynecol J Pelvic Floor Dysfunct. 2000;11:79–83. https://doi.org/10.1007/s001920050074.

6. Kalis V, Karbanova J, Bukacova Z, et al. Anal dilation during labor. Int J Gynecol Obstet. 2010;109:136–9. https://doi.org/10.1016/j.ijgo.2009.11.024.

7. Zemčík R, Karbanova J, Kalis V, et al. Stereophotogrammetry of the perineum during vaginal delivery. Int J Gynecol Obstet. 2012;119:76–80. https://doi.org/10.1016/j.ijgo.2012.05.018.

8. Hoyte L, Damaser MS, Warfield SK, et al (2008) Quantity and distribution of levator ani stretch during simulated vaginal childbirth. Am J Obstet Gynecol 199:198.e1–198.e5. https://doi.org/10.1016/j.ajog.2008.04.027.

9. Parente MPL, Jorge RMN, Mascarenhas T, et al. Deformation of the pelvic floor muscles during a vaginal delivery. Int Urogynecol J. 2007;19:65–71. https://doi.org/10.1007/s00192-007-0388-7.

10. Jing D, Ashton-Miller JA, DeLancey JOL. A subject-specific anisotropic visco-hyperelastic finite element model of female pelvic floor stress and strain during the second stage of labor. J Biomech. 2012;45:455–60. https://doi.org/10.1016/j.jbiomech.2011.12.002.

11. Jansova M, Kalis V, Rusavy Z, et al. Modeling manual perineal protection during vaginal delivery. Int Urogynecol J. 2014;25:65–71. https://doi.org/10.1007/s00192-013-2164-1.

12. Jansova M, Kalis V, Lobovsky L, et al. The role of thumb and index finger placement in manual perineal protection. Int Urogynecol J. 2014;25:1533–40. https://doi.org/10.1007/s00192-014-2425-7.

13. Jansova M, Kalis V, Rusavy Z, et al. Fetal head size and effect of manual perineal protection. PLoS One. 2017;12:e0189842. https://doi.org/10.1371/journal.pone.0189842.

14. Oliveira DA, Parente MPL, Calvo B, et al. A biomechanical analysis on the impact of episiotomy during childbirth. Biomech Model Mechanobiol. 2016;15:1523–34. https://doi.org/10.1007/s10237-016-0781-6.

15. Krofta L, Havelkova L, Urbankova I, et al. Finite element model focused on stress distribution in the levator ani muscle during vaginal delivery. Int Urogynecol J. 2017;28:275–84.

16. Gatellier M-A, dit Gautier EJ, Mayeur O, et al. Complete 3 dimensional reconstruction of parturient pelvic floor. J Gynecol Obstet Hum Reprod. 2020;49:101635. https://doi.org/10.1016/j.jogoh.2019.101635.

17. Parente MP, Natal Jorge RM, Mascarenhas T, et al. Computational modeling approach to study the effects of fetal head flexion during vaginal delivery. Am J Obstet Gynecol. 2010;203:217.e1–6. https://doi.org/10.1016/j.ajog.2010.03.038.

18. Havelková L, Krofta L, Kochová P, et al. Persistent occiput posterior position and stress distribution in levator ani muscle during vaginal delivery computed by a finite element model. Int Urogynecol J. 2020;31:1315–24. https://doi.org/10.1007/s00192-019-03997-8.

19. Bamberg C, Rademacher G, Güttler F, et al. Human birth observed in real-time open magnetic resonance imaging. Am J Obstet Gynecol. 2012;206:505.e1–6. https://doi.org/10.1016/j.ajog.2012.01.011.

20. Ogden RW, Saccomandi G, Sgura I. Fitting hyperelastic models to experimental data. Comput Mech. 2004;34:484–502. https://doi.org/10.1007/s00466-004-0593-y.

21. Kochová P, Cimrman R, Jansová M, et al. The histological microstructure and in vitro mechanical properties of the human female postmenopausal perineal body. Menopause. 2019;26:66–77. https://doi.org/10.1097/GME.0000000000001166.

22. Hsu Y, Chen L, Huebner M, et al. Quantification of levator ani cross-sectional area differences between women with and those without prolapse. Obstet Gynecol. 2006. https://doi.org/10.1097/01.AOG.0000233153.75175.34.

23. Spyrou LA, Aravas N. Muscle and tendon tissues: constitutive modeling and computational issues. J Appl Mech **78**. 2011. https://doi.org/10.1115/1.4003741.

24. Brandão S, Parente M, Mascarenhas T, et al. Biomechanical study on the bladder neck and urethral positions: simulation of impairment of the pelvic ligaments. J Biomech. 2015;48:217–23. https://doi.org/10.1016/j.jbiomech.2014.11.045.

25. Cosson M, Rubod C, Vallet A, et al. Simulation of normal pelvic mobilities in building an MRI-validated biomechanical model. Int Urogynecol J. 2013;24:105–12. https://doi.org/10.1007/s00192-012-1842-8.

26. Long J, Yang J, Lei Z, Liang D. Simulation-based assessment for construction helmets. Comput Methods Biomech Biomed Engin. 2015;18:24–37. https://doi.org/10.1080/10255842.2013.774382.

27. Meriwether KV, Lockhart ME, Meyer I, Richter HE. Anal sphincter anatomy Prepregnancy to Postdelivery among the same Primiparous women on dynamic magnetic resonance imaging. Female Pelvic Med Reconstr Surg. 2019;25:8–14. https://doi.org/10.1097/SPV.0000000000000504.